# Making nonlinear state estimation techniques ready for use in industrial wind turbine control systems

Bastian Ritter[1,3], Axel Schild[2], and Ulrich Konigorski[3]

[1]Industrial Science GmbH, Alexanderstr. 25, 64283 Darmstadt, Germany
[2]IAV GmbH, Rockwellstraße 16, 38518 Gifhorn, Germany
[3]Department of Control Systems and Mechatronics, Technische Universität Darmstadt

## Summary

Nonlinear filter algorithms play an increasing role in advanced multivariable controllers for wind turbine control systems. They are employed to estimate hidden variables and uncertain parameters based on available observations and input signals. The body of research provides a broad range of algorithms which are more or less appropriate for wind turbine application. A practical challenge is the efficient implementation and the testing on industrial target hardware. Another issue is the investigation of observability and identifiability for a given design model to identify potential gains from using non-standard measurement instrumentation. Finally, the illustrative estimation results for the 5-MW reference turbine prove the accuracy and performance of the employed nonlinear filters.

**Keywords:** Nonlinear filters, observability and identifiability analysis, cubature Kalman filter, analysis of measurement configurations, observer architecture

## 1 Introduction

To meet the steadily increasing industrial requirements, wind turbine controllers have reached a mature level of closed-loop performance with respect to energy production and load reduction. These controllers are nonlinear, complex and build heavily upon design heuristics gained from practical experiences. Unfortunately, the latter significantly complicates direct extension of field-proven controllers to new advanced turbine designs without major modifications.

On the other hand, it is even possible to outperform such strong heuristics with advanced multivariable controllers, if only precise information about the dynamic wind turbine state were available. Such information is indeed generated by modern powerful estimation algorithms which handle most practical challenges satisfactorily.

Making these techniques ready for advanced wind turbine applications calls for some basic development steps. At first, the available algorithms must be assessed and implemented incorporating real-time requirements. Secondly, a suitable nonlinear model has to be derived which allows for system analysis including observability and identifiability properties. Since both properties depend strongly on the available instrumentation, a detailed discussion of potential gains in estimation quality is conducted. Furthermore, the filter architecture needs to be implemented both in simulation and on industrial hardware. Finally, the performance assessment and discussion completes the investigation.

## 2 Nonlinear state estimation

State estimation is a central topic for numerous technical and biological applications. Especially advanced state-feedback controllers need the full state information to be accessible in real-time. A major obstacle for the reliable utilization is the requirement not only for accurately known full dynamic state, but also for external disturbances and critical system parameters. Nonlinear Bayesian estimators like sigma-point Kalman filters (SPKF) are a suitable tool to generate these information online with a control-oriented nonlinear turbine model (Sec. 3).

### 2.1 Kalman filter basics

The well-known Kalman filter (KF) has proven to be the optimal filter for linear Gaussian estimation problems [1]. One fundamental prerequisite for applying the KF is a linear (discrete-time) state-space representation of the investigated system defined by

$$\boldsymbol{x}_{k+1} = \mathbf{A}_\mathrm{d}\boldsymbol{x}_k + \mathbf{B}_\mathrm{d}\boldsymbol{u}_k + \boldsymbol{q}_k \tag{1a}$$

$$\boldsymbol{y}_k = \mathbf{C}_\mathrm{d}\boldsymbol{x}_k + \mathbf{D}_\mathrm{d}\boldsymbol{u}_k + \boldsymbol{r}_k \tag{1b}$$

with time-invariant and known system matrices. Secondly, the additive process noise $\boldsymbol{q}_k \sim \mathcal{N}(\mathbf{0}, \mathbf{Q}_k)$ and the measurement noise $\boldsymbol{r}_k \sim \mathcal{N}(\mathbf{0}, \mathbf{R}_k)$ are

assumed to be Gaussian, uncorrelated, zero-mean and white noise sequences [2]. Thus, the state $\boldsymbol{x}_k$ contains a set of $n$ Gaussian random variables (RV). The third condition pertains to the system's property of observability and therefore the question if the complete unknown initial state vector $\boldsymbol{x}_0$ can be inferred uniquely only from known input and observation sequences $\boldsymbol{u}_k$ and $\boldsymbol{y}_k$. Thus, the concept of observability [3] (and identifiability) is discussed in Sec. 4 in detail.

The prediction step of the KF (time update) provides the following a priori estimates for the state vector and its error covariance matrix:

$$\hat{\boldsymbol{x}}_k^- = \mathbf{A}_\mathrm{d}\hat{\boldsymbol{x}}_{k-1}^+ + \mathbf{B}_\mathrm{d}\boldsymbol{u}_{k-1} \tag{2a}$$

$$\mathbf{P}_k^- = \mathbf{A}_\mathrm{d}\mathbf{P}_{k-1}^+\mathbf{A}_\mathrm{d}^\mathrm{T} + \mathbf{Q}_k \quad . \tag{2b}$$

Similarly, applying the correction step (measurement update) yields the posterior estimates:

$$\hat{\boldsymbol{x}}_k^+ = \hat{\boldsymbol{x}}_k^- + \boldsymbol{\mathcal{K}}_k\boldsymbol{v}_k \tag{3a}$$

$$\mathbf{P}_k^+ = \big(\mathbf{I}_n - \boldsymbol{\mathcal{K}}_k\mathbf{C}_\mathrm{d}\big)\mathbf{P}_k^- \quad . \tag{3b}$$

Therein, the observer matrix $\boldsymbol{\mathcal{K}}_k$ (the Kalman gain)

$$\boldsymbol{\mathcal{K}}_k = \mathbf{P}_k^-\mathbf{C}_\mathrm{d}^\mathrm{T}\big(\mathbf{C}_\mathrm{d}\mathbf{P}_k^-\mathbf{C}_\mathrm{d}^\mathrm{T} + \mathbf{R}_k\big)^{-1} \tag{4}$$

serves as a weighting matrix between the predicted state estimate $\hat{\boldsymbol{x}}_k^-$ and the innovation $\boldsymbol{v}_k = \boldsymbol{y}_k - \hat{\boldsymbol{y}}_k$ in order to evaluate the corrected (and improved) state estimate $\hat{\boldsymbol{x}}_k^+$. The innovation sequence, which is the difference between measured and predicted output

$$\hat{\boldsymbol{y}}_k = \mathbf{C}_\mathrm{d}\hat{\boldsymbol{x}}_k^- + \mathbf{D}_\mathrm{d}\boldsymbol{u}_k \quad , \tag{5}$$

injects the new information from observations at time step $k$ to the filter algorithm.

### 2.2 Nonlinear Kalman filters

Despite the existing rich body of theory and free-of-charge academic tools, nonlinear state estimation has so far received only little attention in the wind energy community. For nonlinear systems (like wind turbines), which are usually on hand as state-space systems like

$$\boldsymbol{x}_{k+1} = \boldsymbol{f}_\mathrm{d}(\boldsymbol{x}_k, \boldsymbol{u}_k, \boldsymbol{\theta}_k) + \boldsymbol{q}_k \tag{6a}$$

$$\boldsymbol{y}_k = \boldsymbol{h}_\mathrm{d}(\boldsymbol{x}_k, \boldsymbol{u}_k, \boldsymbol{\theta}_k) + \boldsymbol{r}_k \quad , \tag{6b}$$

there exist a variety of filter algorithms which provide better estimates in the Gaussian but also in the non-Gaussian framework than the linear KF [4].

The established standard local filter is the extended Kalman filter (EKF) which builds on a recursive linearisation procedure of the nonlinear system model in Eqs. (6). Despite the known major drawback of filter divergence [5] it is still used in many applications due to its simplicity and straightforward implementation coming from the linear KF algorithm.

However, in 1997 the invention of the unscented Kalman filter (UKF) has launched the development of a new class of derivative-less local filters [6]. These algorithms are today summarized within the framework of sigma-point Kalman filters (SPKF).

Other than the EKF, all SPKF avoid in general the numerical computation of partial derivatives to obtain a linearised mapping of the system dynamics. Thus, rather than linearising the known nonlinear model, the SPKF approximate the multivariate probability density functions by a set of deterministically chosen sigma-points ($\boldsymbol{\mathcal{S}_\mathcal{P}}$). These $\boldsymbol{\mathcal{S}_\mathcal{P}}$ are passed through the nonlinear model and to obtain thereafter an improved Gaussian approximation for the statistical properties of the transformed $\boldsymbol{\mathcal{S}_\mathcal{P}}$. The many variants of filters differ mainly by the number of $\boldsymbol{\mathcal{S}_\mathcal{P}}$ and the choice of their associated weights.

The new class of SPKF includes besides the UKF also the central-difference Kalman filter (CDKF), the Gauss-Hermite Kalman filter (GHKF) and the cubature Kalman filter (CKF) - as the latest family member [7]. The theory of UKF and CDKF has already been assessed by various publications for other technical applications [5, 8, 9, 10].

In contrast, the CKF has rarely been discussed at all and until now never (to the author's knowledge) for wind turbine application. Due to this gap, the paper discusses in the next section the CKF implementation and highlights in addition some practical advantages over the UKF.

### 2.3 Efficient cubature Kalman filters

For the above nonlinear Gaussian estimation problems the Kalman filter Eqs. (2 - 4) have to be modified in order to incorporate the nonlinear system dynamics. To obtain these relations, the CKF employs a spherical-radial cubature rule to evaluate the multivariate probability distributions (while e.g. the UKF uses the unscented transformation).

Since emphasis is put on an efficient and a robust implementation, we skip the standard version of the CKF and directly aim at the square-root cubature Kalman filter (SRCKF). Thus, instead of the error covariance matrix $\mathbf{P}_k$ its matrix square-root or Cholesky factor $\mathbf{S}_k$ is directly computed by the filter algorithm. Both matrices are related by $\mathbf{P}_k = \mathbf{S}_k\mathbf{S}_k^\mathrm{T}$ where $\mathbf{S}_k$ is a lower triangular matrix.

The CKF uses $2n$ sigma-points (or cubature points) which propagate the stochastic properties of the state through the nonlinear model. This is one $\boldsymbol{\mathcal{S}_\mathcal{P}}$ less than the UKF which is important for the filter's robustness. Since the first $\boldsymbol{\mathcal{S}_\mathcal{P}}$ as the mean of the set may have a large negative weight, the resulting covariance matrix may not always be positive definit. Thus, the square-root UKF needs in general several Cholesky downdates on the matrix square-root $\mathbf{S}_k^+$ in every recursion step. Moreover, the CKF has only the noise covariances $\mathbf{Q}_k$ and $\mathbf{R}_k$ as free design parameters (while the UKF needs three addi-

tional parameters which must be chosen properly). Despite this, the CKF shows the same accuracy as the UKF in simulations and has therefore mainly numerical advantages.

The algorithm of the SRCKF is separated into a prediction step 1 and a correction step 2 as follows:

1a) Compute $2n$ sigma-points and propagate them through the nonlinear state equation:

$$\boldsymbol{\mathcal{X}}_{k-1}^{+} = \hat{\mathbf{X}}_{k-1}^{+} + \sqrt{n}\,\big[\mathbf{S}_{k-1}^{+}\ ,\ -\mathbf{S}_{k-1}^{+}\big] \tag{7a}$$

$$\boldsymbol{\mathcal{X}}_{k}^{*} = \boldsymbol{f}_{\mathrm{d}}(\boldsymbol{\mathcal{X}}_{k-1}^{+}, \mathbf{U}_{k-1}) \tag{7b}$$

1b) Evaluate the a priori state estimate and the Cholesky factor of the covariance matrix by QR decomposition:

$$\hat{\boldsymbol{x}}_{k}^{-} = \frac{1}{2n}\sum_{i=1}^{2n} \boldsymbol{\mathcal{X}}_{k}^{*}(:,i) \tag{8a}$$

$$\mathbf{S}_{k}^{-} = qr\Big\{\Big[\tfrac{1}{\sqrt{2n}}\big(\boldsymbol{\mathcal{X}}_{k}^{*} - \hat{\mathbf{X}}_{k}^{-}\big)\ ,\ \mathbf{S}_{\mathrm{Q},k}\Big]\Big\} \tag{8b}$$

2a) Compute $2n$ new sigma-points and propagate them through the measurement equation:

$$\boldsymbol{\mathcal{X}}_{k}^{-} = \hat{\mathbf{X}}_{k}^{-} + \sqrt{n}\,\big[\mathbf{S}_{k}^{-}\ ,\ -\mathbf{S}_{k}^{-}\big] \tag{9a}$$

$$\boldsymbol{\mathcal{Y}}_{k}^{*} = \boldsymbol{h}_{\mathrm{d}}(\boldsymbol{\mathcal{X}}_{k}^{-}, \mathbf{U}_{k}) \tag{9b}$$

2b) Evaluate the predicted output and the matrix square-root of the innovation covariance:

$$\hat{\boldsymbol{y}}_{k} = \frac{1}{2n}\sum_{i=1}^{2n} \boldsymbol{\mathcal{Y}}_{k}^{*}(:,i) \tag{10a}$$

$$\mathbf{S}_{\mathrm{y},k} = qr\Big\{\Big[\tfrac{1}{\sqrt{2n}}\big(\boldsymbol{\mathcal{Y}}_{k}^{*} - \hat{\mathbf{Y}}_{k}\big)\ ,\ \mathbf{S}_{\mathrm{R},k}\Big]\Big\} \tag{10b}$$

2c) Calculate the error cross-covariance matrix and then evaluate (update) the Kalman gain:

$$\mathbf{P}_{xy,k} = \frac{1}{2n}\big(\boldsymbol{\mathcal{X}}_{k}^{-} - \hat{\mathbf{X}}_{k}^{-}\big)\big(\boldsymbol{\mathcal{Y}}_{k}^{*} - \hat{\mathbf{Y}}_{k}\big)^{\mathrm{T}} \tag{11a}$$

$$\boldsymbol{\mathcal{K}}_{k} = \big(\mathbf{P}_{xy,k}/\mathbf{S}_{\mathrm{y},k}^{\mathrm{T}}\big)/\mathbf{S}_{\mathrm{y},k} \tag{11b}$$

2d) Compute a posterior state estimate and covariance matrix square-root by QR decomposition

$$\hat{\boldsymbol{x}}_{k}^{+} = \hat{\boldsymbol{x}}_{k}^{-} + \boldsymbol{\mathcal{K}}_{k}\boldsymbol{v}_{k} \tag{12a}$$

$$\mathbf{S}_{k}^{+} = qr\big\{\big[\boldsymbol{\mathcal{Z}}_{k}\ ,\ \boldsymbol{\mathcal{K}}_{k}\mathbf{S}_{\mathrm{R},k}\big]\big\} \tag{12b}$$

where $\boldsymbol{\mathcal{Z}}_{k}$ is defined by

$$\boldsymbol{\mathcal{Z}}_{k} = \frac{1}{\sqrt{2n}}\Big(\big(\boldsymbol{\mathcal{X}}_{k}^{-} - \hat{\mathbf{X}}_{k}^{-}\big) - \boldsymbol{\mathcal{K}}_{k}\big(\boldsymbol{\mathcal{Y}}_{k}^{*} - \hat{\mathbf{Y}}_{k}\big)\Big) \quad . \tag{13}$$

Comparing these equations with the linear KF, the complexity of the algorithm obviously increases significantly. However, the CKF is now applicable for arbitrary (including non-differentiable) nonlinear systems which is a great improvement in comparison to the EKF. This benefit results from the functional evaluations which are executed for the nonlinear model in Eqs. (7b) and (9b).

In a nutshell, the design equations become a lot more complicated, but the free design parameters of the filter, $\mathbf{Q}_k$ and $\mathbf{R}_k$ (or its associated Cholesky factors $\mathbf{S}_{\mathrm{Q},k}$ and $\mathbf{S}_{\mathrm{R},k}$), remain the same. As can be seen from the above equations, a nonlinear plant representation is necessary as an internal design model for the algorithm. Such models will be introduced in the next section.

## 3 Modeling of wind turbine dynamics

The design model must be tailored to the specific problem. Thus, a control engineer must match the model granularity to the control and/or estimation task which he or she wants to solve [4]. Unlike higher order simulation models such as FASTv8, Flex5 and Bladed, the (internal) controller and/or state estimator design model must be of reduced order to be feasible and yet simple to comprehend.

Since the advanced design model in Eq. (15) is too complex to introduce it in detail in this paper, the following simplified wind turbine drive-train model

$$\ddot{\varphi}_{\mathrm{g}} = \frac{\rho}{2}\frac{\pi R^3}{\Theta} C_{\mathrm{M}}\Big(\frac{\dot{\varphi}_{\mathrm{g}} R}{v_{\mathrm{w}}}, \beta\Big)\, v_{\mathrm{w}}^2 - \frac{i_{\mathrm{gb}}}{\Theta} M_{\mathrm{g}} \tag{14a}$$

$$n_{\mathrm{g}} = \frac{60}{2\pi} i_{\mathrm{gb}}\, \dot{\varphi}_{\mathrm{g}} \tag{14b}$$

is considered for illustrative purposes. Eq. (14a) represents the known torque balance on the rotor side and Eq. (14b) the observation model. The following vector quantities are defined: The dynamic state vector $\boldsymbol{x} = [\dot{\varphi}_{\mathrm{g}}]$, the control input $\boldsymbol{u} = [M_{\mathrm{g}}\ \beta]^{\mathrm{T}}$, the disturbance input $\boldsymbol{d} = [v_{\mathrm{w}}]$, the parameter vector $\boldsymbol{\theta} = [\rho]$ and the output vector $\boldsymbol{y} = [n_{\mathrm{g}}]$. The remaining model parameters are assumed to be constant and a priori known. The aerodynamic torque coefficient $C_{\mathrm{M}}(\lambda, \beta)$ for the NREL 5-MW turbine is shown in Fig. 1.

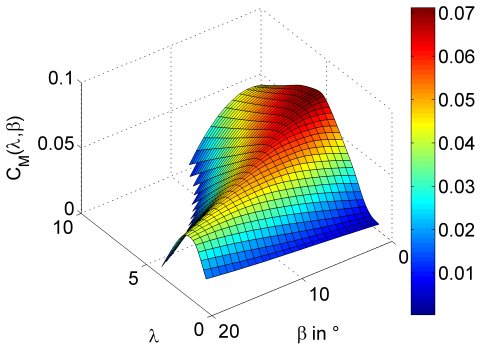


Fig. 1: Aerodynamic torque coefficient

Such a model is well suited to estimate the rotor effective wind speed only from the knowledge of the input $\boldsymbol{u}$ and the output $\boldsymbol{y}$. This task is relatively simple and the wind speed is observable even without

incorporating the wind anemometer. Yet, the more sophisticated (and quite interesting practical) question raised by engineers reads:

Is it possible to estimate $\boldsymbol{x}$, $\boldsymbol{d}$ and $\boldsymbol{\theta}$ simultaneously and uniquely from observations? And if so, what conditions apply? The answer provides a detailed structural observability analysis (Sec. 4.1).

Apart from the rather simple model in Eq. (14), a more complex model including nacelle and drivetrain dynamics has been established for state and parameter estimation purposes in [4, 11]. Aiming at a thorough observability analysis as well as a detailed investigation of benefits from additional measurements, this model is augmented by the relevant out-of-plane blade dynamics.

Hence, the considered wind turbine model for the detailed analysis in Sec. 4.2 consists of 14 mechanical states and is defined by the following set of nonlinear second-order differential equations:

$$\begin{aligned}
\ddot{x}_{\mathrm{T}} &= f_1\big(\boldsymbol{x},\boldsymbol{u},\boldsymbol{\theta},\boldsymbol{d}\big)\\
\ddot{y}_{\mathrm{T}} &= f_2\big(\boldsymbol{x},\boldsymbol{u},\boldsymbol{\theta},\boldsymbol{d}\big)\\
\ddot{\varphi}_{\mathrm{g}} &= f_3\big(\boldsymbol{x},\boldsymbol{u},\boldsymbol{\theta},\boldsymbol{d}\big)\\
\Delta\ddot{\varphi} &= f_4\big(\boldsymbol{x},\boldsymbol{u},\boldsymbol{\theta},\boldsymbol{d}\big)\\
\ddot{x}_{\mathrm{B},1} &= f_5\big(\boldsymbol{x},\boldsymbol{u},\boldsymbol{\theta},\boldsymbol{d}\big)\\
\ddot{x}_{\mathrm{B},2} &= f_6\big(\boldsymbol{x},\boldsymbol{u},\boldsymbol{\theta},\boldsymbol{d}\big)\\
\ddot{x}_{\mathrm{B},3} &= f_7\big(\boldsymbol{x},\boldsymbol{u},\boldsymbol{\theta},\boldsymbol{d}\big) \quad .
\end{aligned} \tag{15}$$

These dynamic equations can always be reformulated and collected in the state vector equation

$$\dot{\boldsymbol{x}} = \boldsymbol{f}(\boldsymbol{x},\boldsymbol{u},\boldsymbol{\theta},\boldsymbol{d}) \quad \in \mathbb{R}^{14} \tag{16}$$

as first part of the nonlinear state-space model. Still, without the measurement vector equation this representation is not complete. The choice of the outputs also directly affects the amount of information about a desired hidden quantity. Thus, in order to assess these effects of the measurement instrumentation on the observability properties, the following three configurations are investigated:

a) The standard measurement instrumentation includes axial and lateral nacelle accelerations, the generator speed and rotor azimuth angle:

$$\boldsymbol{y}_{\mathrm{std}} = \big[\ddot{x}_{\mathrm{T}}\ \ddot{y}_{\mathrm{T}}\ n_{\mathrm{g}}\ \varphi\big]^{\mathrm{T}} \in \mathbb{R}^4. \tag{17}$$

b) The extended measurement instrumentation includes additionally the three individual out-of-plane blade-root bending moments:

$$\boldsymbol{y}_{\mathrm{ext}} = \big[\ \cdots\ M_{\mathrm{By},1}\ M_{\mathrm{By},2}\ M_{\mathrm{By},3}\big]^{\mathrm{T}} \in \mathbb{R}^7. \tag{18}$$

c) The advanced instrumentation considers also the tower base bending moments:

$$\boldsymbol{y}_{\mathrm{adv}} = \big[\ \cdots\ M_{\mathrm{Tx}}\ M_{\mathrm{Ty}}\big]^{\mathrm{T}} \in \mathbb{R}^9. \tag{19}$$

Hence, the information about the system states and parameters (contained in the observed output vector) should gradually increase from standard to extended to advanced configuration. This assumption will be analysed by an observability and identifiability analysis.

## 4 Observability and identifiability

The concepts of observability and identifiability are actually two different approaches to assess (physical) properties of a dynamic state-space model in a systematic way. Both concepts attempt to identify and evaluate the amount of information about a particular quantity in the measurable output.

While observability is always related to system states $\boldsymbol{x}$, the concept of identifiability focuses on the constant parameters $\boldsymbol{\theta}$ and on the disturbance inputs $\boldsymbol{d}$ (which can be interpreted as quickly time-varying parameters).

Considering linear systems like (1), observability depends only on the system matrices ($\mathbf{A}_{\mathrm{d}}$ and $\mathbf{C}_{\mathrm{d}}$), and is evaluated for instance with Kalman's observability criterion or the observability gramian matrix [12]. Thus, the specific control input $\boldsymbol{u}$ is irrelevant to evaluate if all states are uniquely observable. On the contrary, identifiability depends in general on the (control and disturbance) input signals because the identification problem is nonlinear also for linear state-space models. For this reason, a persistent excitation by the system inputs must be enforced to identify system parameters.

In case of nonlinear systems, both observability and identifiability cannot be strictly separated any more since both are in general dependent on the input and moreover, states and parameters are related arbitrarily. Both concepts can then be tackled together if the state vector of original system is augmented by the parameters which yields

$$\boldsymbol{x}_a^{\mathrm{T}} = \big[\boldsymbol{x}^{\mathrm{T}}\ \boldsymbol{\theta}^{\mathrm{T}}\ \boldsymbol{d}^{\mathrm{T}}\big] \quad . \tag{20}$$

Since there is mathematically no difference between physical and fictitious states (parameters) the state Eq. (16) turns formally into

$$\dot{\boldsymbol{x}}_a = \boldsymbol{f}_a(\boldsymbol{x}_a,\boldsymbol{u}) \tag{21}$$

assuming the following dynamic parameter models

$$\dot{\boldsymbol{\theta}} = \mathbf{0} \qquad \text{and} \qquad \dot{\boldsymbol{d}} = \mathbf{0} \quad . \tag{22}$$

Thus, identifiability is assessed indirectly by investigating the observability of the augmented states.

There are mainly two approaches to investigate identifiability [13]:

1. The theoretical or structural identifiability and
2. the practical local identifiability analysis including sensitivity-based methods.

In this contribution we focus first on the theoretical analysis in Sec. 4.1 and highlight after that the practical concepts in Sec. 4.2. The latter are also applicable for higher order nonlinear systems as they assess the identifiability locally based on either experimental or simulation data. An overview on definitions and concepts on identifiability analysis is given by [13, 14].

### 4.1 Structural identifiability analysis

The theoretical analysis of observability and identifiability is often very hard to conduct and sometimes impossible for nonlinear systems. Still, we will show in the following how this procedure is conducted in principle employing the illustrative model from Eq. (14). After augmenting the states and performing some generalizations, the following state-space representation is obtained

$$\begin{bmatrix}\dot{x}_1\\ \dot{x}_2\\ \dot{x}_3\end{bmatrix}=\begin{bmatrix}p_1\,x_3\,f\big(\frac{x_1\,p_2}{x_2},u_2\big)\,x_2^2+p_3\,u_1\\ 0\\ 0\end{bmatrix} \tag{23a}$$

$$y=p_4\,x_1 \tag{23b}$$

where $p_4$ is set to 1 without loss of generality (if $p_4=0$ as trivial case is excluded). Then, one possibility to prove the global and structural identifiability is to show that the following mapping

$$\boldsymbol{z}=\begin{bmatrix}y\\ \dot{y}\\ \ddot{y}\end{bmatrix}=\begin{bmatrix}x_1\\ p_1\,x_3\,f\big(\frac{x_1\,p_2}{x_2},u_2\big)\,x_2^2+p_3\,u_1\\ p_1\,x_3\,\dot{f}\big(\frac{x_1\,p_2}{x_2},u_2\big)\,x_2^2+p_3\,\dot{u}_1\end{bmatrix} \tag{24}$$

is invertible with respect to $\boldsymbol{x}$. However, this is not possible for an arbitrary function $f(x_1/x_2,u_2)$. Restricting ourselves to the partial load operating regime and thus $u_2=0$, such general statements on identifiability can be obtained from Eq. (24). In addition, the solution may serve as a simple state estimator which will be discussed in future contributions. Anyhow, the time derivative

$$\dot{f}\Big(\frac{x_1\,p_2}{x_2},u_2\Big)=\frac{\partial f}{\partial x_1}\dot{x}_1+\frac{\partial f}{\partial x_2}\dot{x}_2+\frac{\partial f}{\partial u_2}\dot{u}_2 \tag{25}$$

must not be equal to zero in general and thus either $\dot{u}_1\neq 0$ or $\dot{u}_2\neq 0$ must hold. Therefore, if the system approaches steady-state conditions, identifiability is lost in any case since Eq. (24) can then never be solved for $\boldsymbol{x}$. Due to the fact that the nonlinear mapping $\boldsymbol{z}=\boldsymbol{q}(\boldsymbol{x},\boldsymbol{u})$ is rarely invertible dealing with wind turbines dynamics,

$$\boldsymbol{x}=\boldsymbol{q}^{-1}(y,\dot{y},\ddot{y},\boldsymbol{u},\dot{\boldsymbol{u}}) \tag{26}$$

often cannot be derived explicitly. Nevertheless, the practical local observability may be still assessed by computing the following Jacobian matrix

$$\boldsymbol{Q}(\boldsymbol{x},\boldsymbol{u},\dot{\boldsymbol{u}})=\frac{\partial \boldsymbol{z}}{\partial \boldsymbol{x}}\quad . \tag{27}$$

Investigating the rank of $\boldsymbol{Q}$ numerically for a given wind turbine and simulation data proves that this local observability matrix has full rank provided $x_2>0$ and $x_3\neq 0$. Thus, the engineer can draw the following conclusions: As the wind speed $x_2=v_\mathrm{w}$ is non-zero during operation and the air density $x_3=\rho$ as well, the only restriction to obtain unique estimates for the three augmented states is that the inputs must be persistently exciting the dynamic system.

This discussion shows that even for simple wind turbine models the theoretical observability and identifiability analysis can become tough rather quickly. Thus, practical numerical tools are required e.g. based on Fisher Information which is discussed in the next section.

### 4.2 Sensitivity analysis

There are several practical tools to investigate the local observability of nonlinear systems based on a sensitivity analysis [14, 15]. In this paper we employ and investigate the local observability Gramian matrix $\mathbf{G}$ defined as follows:

$$\mathbf{G}=\int_0^{T_0}\mathbf{\Phi}^\mathrm{T}(t)\mathbf{C}^\mathrm{T}(t)\mathbf{C}(t)\mathbf{\Phi}(t)\mathrm{d}t \tag{28}$$

where $\mathbf{\Phi}(t)$ is the state transition matrix and $\mathbf{C}(t)$ the output matrix. The Gramian matrix $\mathbf{G}$ is evaluated for the time interval $T_0$ for the local linear model containing the information about the observability of states and parameters within its singular values. From a practical point of view the empirical observability Gramian [14] is assessed which is easier to compute than $\mathbf{\Phi}(t)$ and $\mathbf{C}(t)$ at each time step in Eq. (28).

The analysis of the empirical Gramian observability matrix is conducted for the same simulation results used in the next section. The evaluation of the eigenvalues and eigenvectors provides quantitative observability measures [14]. These criteria are computed for the three different measurement configurations introduced in Sec. 3.

First, the comparison of standard and extended configuration is shown in Fig. 2. It shows the change of observability for the 28 augmented states (14 mechanical, 2 disturbance inputs and 12 parameters). The states and parameters related to the nacelle and drive-train dynamics are not affected by the additional outputs. The observability measure is for most of them bigger than $10^{-3}$ which features good conditions for estimation. A significant improvement can be observed for the blade deflections and some parameters of the blade model.

In contrast to Fig. 2, the comparison of extended and advanced measurement configuration in Fig. 3 indicates insignificant changes of observability conditions (except for one parameter related to the turbine height). Thus, the content of information in the output vector obviously does not increase although

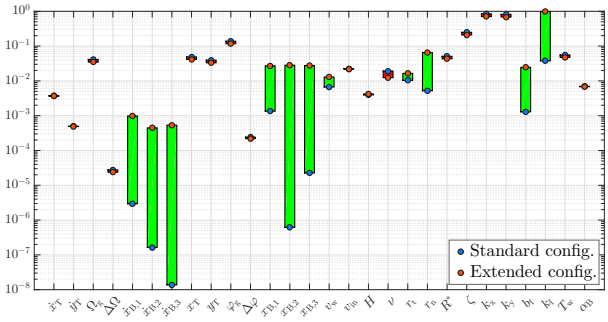


Fig. 2: Change of empirical Gramian observability measures (standard vs. extended configuration). The green bars indicate improvements in observability.

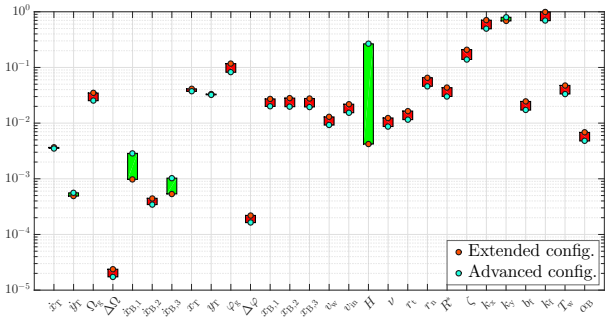


Fig. 3: Change of the empirical Gramian observability measure (extended vs. advanced configuration)

there are more observations available. This indicates redundancy in the measurement instrumentation. As final remark to Fig. 3, the states related to the drive-train torsion ($\Delta\Omega$ and $\Delta\varphi$) have the lowest observability measures. This correlates with the estimation results for drive-train torsion in Fig. 5.

Since there is no sustainable benefit from using the advanced measurement instrumentation it is excluded from the further investigation.

In summary, the observability analysis has revealed vital properties for a successful practical application of nonlinear filters. The discussed observability criteria allow also for detection of good conditions to estimate critical system parameters during operation which is indispensable for an online model update.

## 5 Simulation and hardware test results

In the previous sections several important aspects related to nonlinear state estimation have been discussed. The knowledge gained from this investigation is condensed now into the design of advanced estimators for wind turbine application.

### 5.1 Simulation results from aeroelastic code

The observability analysis provided the theoretical background to investigate different measurement configurations. Since the advanced configuration has no major benefit compared to the extended configuration, it is excluded from the following considerations.

The SRCKF algorithms have been implemented and assessed for both configurations in Matlab/Simulink. These observers are tested with the 5-MW onshore reference wind turbine [16] using the Simulink interface to the complex nonlinear simulator FASTv8 [17]. The choice of the filter design parameters is beyond the scope of this paper and therefore excluded.

The illustrative estimation results are obtained for a turbulent wind field in the full load regime (generated according to the standard IEC-61400). Fig. 4 shows the effective wind speed, the generator power, the control inputs and the observed outputs with different measurement noise levels. As expected the controller provides the nominal electrical power of 5 MW.

With the known control inputs and the noisy measurements the nonlinear filters estimate the critical states and parameters which is presented in Fig. 5. The following general observations are made:

1. The filter performance to estimate the nacelle dynamics is very accurate. It is similar for standard and extended measurement configuration.
2. The drive-train dynamics are assessable without direct load measurements.
3. The wind speed is observed with high precision despite the fact that no measurable wind information is assumed to be available for the filter. A small time delay appears due to the delayed effect on the drive-train and nacelle dynamics.
4. The main difference between standard and extended measurement equipment arises for the blade dynamic response. This correlates also with the results obtained from observability analysis.
5. The blade deflection can be predicted accurately based on information of the extended measurement configuration.

The estimation results confirm that the standard instrumentation (available in every modern wind turbine) is sufficient to generate accurate estimates of unmeasurable or hidden quantities. These information can be provided to advanced state-feedback controllers to improve closed-loop performance [18].

Significant improvements arise from extended configuration mainly for estimation of system states and parameters related to the blade dynamics.

### 5.2 Implementation on industrial hardware

As highlighted in [4] the estimation problem consists of multiple sub-problems including state, parameter and load estimation. If real-time application is critical, these sub-problems can be tackled by an efficient observer architecture (Fig. 6). By this means

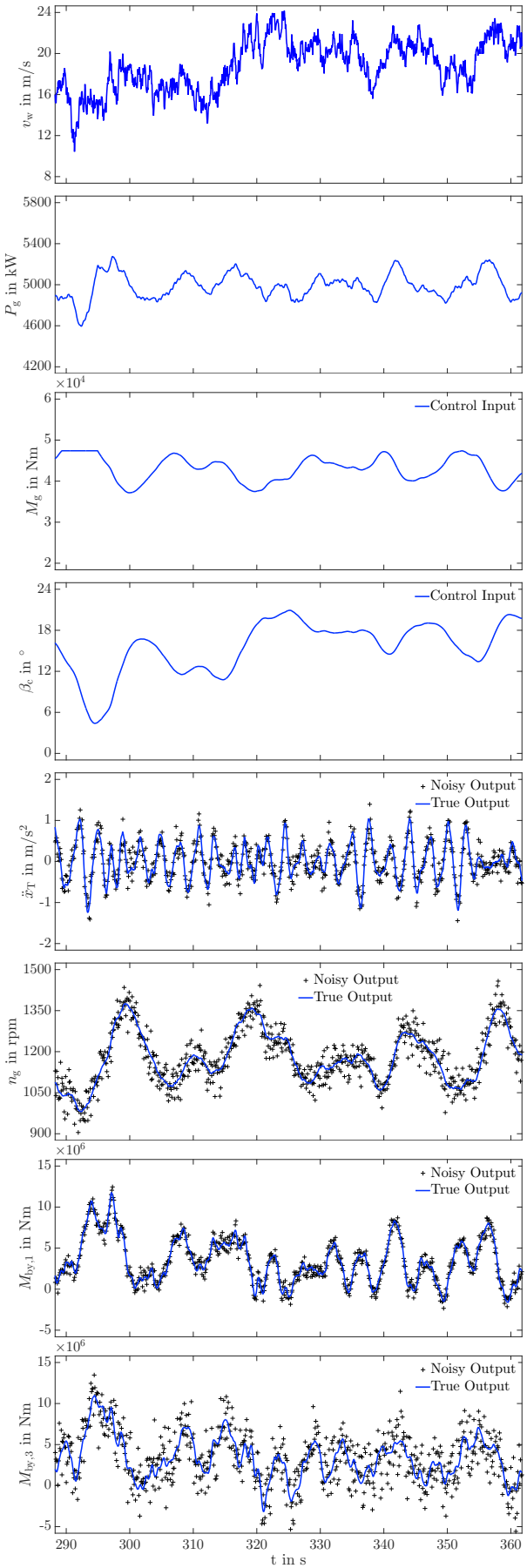


Fig. 4: Comparison of control inputs, disturbance inputs and measurement outputs

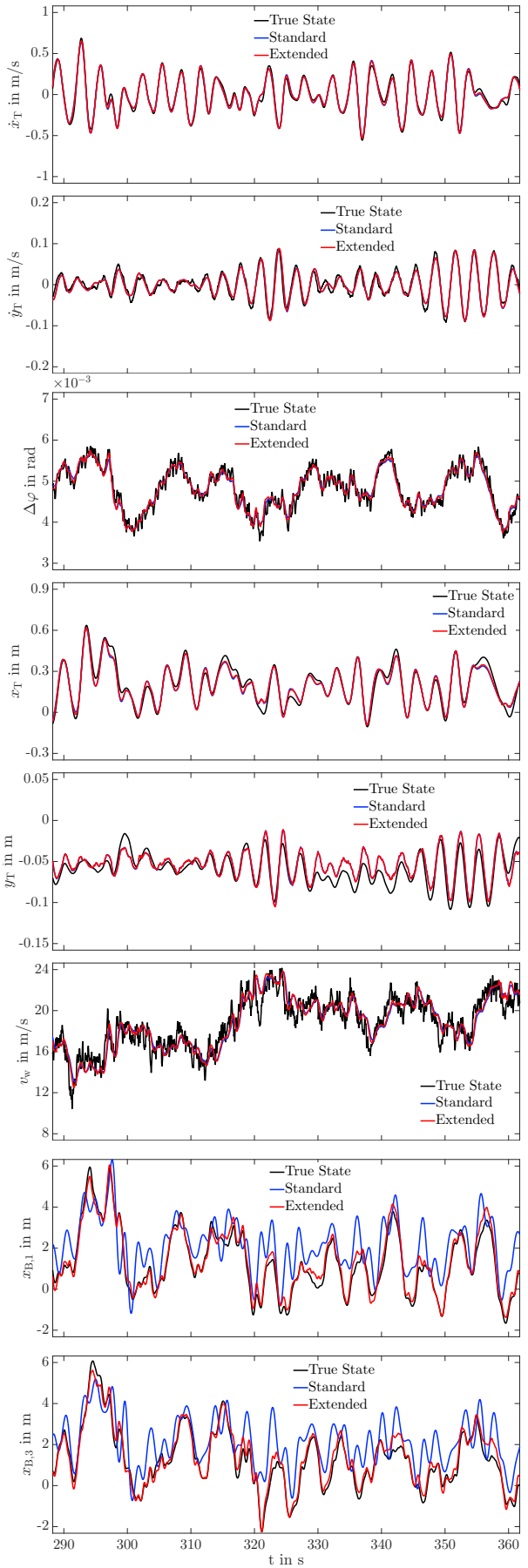


Fig. 5: Comparison of results from standard vs. extended configuration for state and parameter estimation

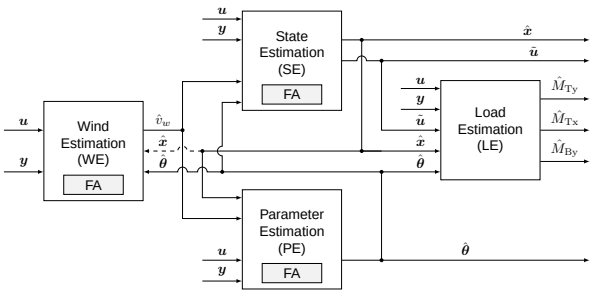


Fig. 6: Structural sketch of observer architecture

the system properties can be exploited to save computational effort. Moreover, such a distributed architecture enables to use different linear and nonlinear filter types suited to the sub-problems. Further advantages are the selective filter adaptation (e.g. for the wind estimator) and the situational by-passing triggered by (online) observability measures.

Since the testing of controller and observer performance in simulation has provided very promising results, the question of hardware implementation must be addressed subsequently. Therefore, the Beckhoff controller CX2040 has been chosen as a reference of a state-of-the-art industrial controller.

The SRCKF and various other filter algorithms were successfully tested and implemented in Matlab/Simulink in the first place. These filters have been exported via Simulink code generation and TwinCat3 to the industrial controller.

The hardware study was then conducted with the 28th order nonlinear model which required a computational time of less than 10 ms for each recursion step (using monolithic sigma-point filter algorithms). A significant improvement on that was possible by deploying the right observer architecture as briefly discussed above.

## 6 Conclusions

The investigation of powerful recursive nonlinear algorithms for state estimation of wind turbines proves to be real-time feasible already. This has been demonstrated by estimation results for the NREL 5-MW reference turbine and additional hardware testing on a state-of-the-art industrial controller. The observability and identifiability analysis provided new information relevant especially for successful application of nonlinear state estimators in the field. Furthermore, a quantitative evaluation of the benefits from non-standard measurements has been conducted which proved the significant potential for both estimation quality and control performance incorporating blade root sensors. The body of research yet provides all required features to successfully tackle the practical challenges like robustness of implementation and constraint-handling. The main challenge remaining is the successful integration into an industry-ready platform and the field testing on real wind turbines.

## References


[1] R. E. Kalman, “A new approach to linear filtering and prediction problems,” *Trans. ASME - Journal of Basic Engineering*, vol. 82, no. D, 1960.

[2] D. Simon, *Optimal State Estimation. Kalman, $H_\infty$, and Nonlinear Approaches*. John Wiley & Sons, 2006.

[3] E. G. Gilbert, “Controllability and observability in multivariable control systems,” *SIAM Control*, vol. 2, no. 1, pp. 128–151, 1963.

[4] B. Ritter, A. Schild, M. Feldt, and U. Konigorski, “The design of nonlinear observers for wind turbine dynamic state and parameter estimation,” *Journal of Physics: Conference Series*, 2016.

[5] E. A. Wan and R. van der Merwe, “The unscented kalman filter for nonlinear estimation,” *IEEE Symposium 2000 (AS-SPCC)*, 2000.

[6] S. J. Julier and J. K. Uhlmann, “A new extension of the kalman filter to nonlinear systems,” *11th International symposium on Aerospace/Defence Sensing, Simulation and Control*, 1997.

[7] I. Arasaratnam and S. Haykin, “Cubature kalman filters,” *IEEE Transactions on Automatic Control*, vol. 54, no. 6, pp. 1254–1269, June 2009.

[8] R. van der Merwe, “Sigma-point kalman filters for probabilistic inference in dynamic state-space models,” Ph.D. dissertation, OGI School of Science & Engineering at Oregon Health & Science University, 2004.

[9] K. Ito and K. Xiong, “Gaussian filters for nonlinear filtering problems,” *IEEE Trans. Autom. Control*, vol. 45, no. 5, pp. 910–927, 05 2000.

[10] Y. Wu, D. Hu, M. Wu, and X. Hu, “Unscented kalman filtering for additive noise case: Augmented versus nonaugmented,” *IEEE Signal Processing Letters*, vol. 12, no. 5, p. 4, 05 2005.

[11] B. Ritter, H. Fürst, U. Konigorski, and M. Eichhorn, “Multivariable model for simulation and control design of wind turbines,” *Proceedings of the 12th German Wind Energy Conference (DEWEK)*, 2015.

[12] S. Skogestad and I. Postlethwaite, *Multivariable Feedback Control. Analysis and Design*, 1st ed. John Wiley & Sons, 2001.

[13] H. Miao, X. Xia, A. S. Perelson, and H. Wu, “On identifiability of nonlinear ode models and applications in viral dynamics,” *SIAM Rev Soc Ind Appl Math.*, vol. 53, no. 1, pp. 3–39, January 2011.

[14] A. J. Krener and K. Ide, “Measures of unobservability,” 2009.

[15] T. Quaiser and M. Mönnigmann, “Systematic identifiability testing for unambiguous mechanistic modeling - application to jak-stat, map kinase, and nf-k b signaling pathway models,” *BMC System Biology*, vol. 3, no. 50, pp. 50–71, January 2009.

[16] J. Jonkman, S. Butterfield, W. Musial, and G. Scott, “Definition of a 5-mw reference wind turbine for offshore system development,” National Renewable Energy Laboratory (NREL), Tech. Rep. Technical Report NREL/TP-500-38060 February 2009, 2009.

[17] J. Jonkman and B. Jonkman. (2015) Nwtc information portal (fast v8). https://nwtc.nrel.gov/fast8.

[18] B. Ritter and U. Konigorski, “Advanced multivariable control design for modern multi-mw wind turbines,” *Proceedings of the 11th EAWE PhD Seminar on Wind Energy in Europe*, 2015.

## Nomenclature

| | | |
|---|---|---|
| $n$ | $\in \mathbb{Z}$ | number of states |
| $\boldsymbol{x}_k$ | $\in \mathbb{R}^n$ | dynamic state vector |
| $\hat{\boldsymbol{x}}_k^-$ | $\in \mathbb{R}^n$ | a priori state estimate |
| $\hat{\boldsymbol{x}}_k^+$ | $\in \mathbb{R}^n$ | posterior state estimate |
| $\boldsymbol{u}_k$ | $\in \mathbb{R}^p$ | control input vector |
| $\boldsymbol{d}_k$ | $\in \mathbb{R}^d$ | disturbance input vector |
| $\boldsymbol{\theta}_k$ | $\in \mathbb{R}^r$ | parameter vector |
| $\boldsymbol{v}_k$ | $\in \mathbb{R}^q$ | innovation sequence |
| $\boldsymbol{y}_k$ | $\in \mathbb{R}^q$ | observed system output vector |
| $\hat{\boldsymbol{y}}_k$ | $\in \mathbb{R}^q$ | predicted system output vector |
| $\mathbf{A}_\mathrm{d}$ | $\in \mathbb{R}^{n\times n}$ | system matrix |
| $\mathbf{B}_\mathrm{d}$ | $\in \mathbb{R}^{n\times p}$ | control input matrix |
| $\mathbf{C}_\mathrm{d}$ | $\in \mathbb{R}^{q\times n}$ | observation output matrix |
| $\mathbf{D}_\mathrm{d}$ | $\in \mathbb{R}^{q\times p}$ | direct feedthrough matrix |
| $\mathbf{I}_n$ | $\in \mathbb{R}^{n\times n}$ | unity matrix |
| $\boldsymbol{\mathcal{K}}_k$ | $\in \mathbb{R}^{n\times q}$ | Kalman gain matrix |
| $\mathbf{P}_k^-$ | $\in \mathbb{R}^{n\times n}$ | a priori state error covariance matrix |
| $\mathbf{P}_k^+$ | $\in \mathbb{R}^{n\times n}$ | posterior state error covariance matrix |
| $\mathbf{P}_{xy,k}$ | $\in \mathbb{R}^{n\times q}$ | error cross-covariance matrix |
| $\mathbf{Q}_k$ | $\in \mathbb{R}^{n\times n}$ | process noise covariance matrix |
| $\mathbf{R}_k$ | $\in \mathbb{R}^{q\times q}$ | measurement noise covariance matrix |
| $\mathbf{S}_{\mathrm{Q},k}$ | $\in \mathbb{R}^{n\times n}$ | Cholesky factor of $\mathbf{Q}_k = \mathbf{S}_{\mathrm{Q},k}\mathbf{S}_{\mathrm{Q},k}^\mathrm{T}$ |
| $\mathbf{S}_{\mathrm{R},k}$ | $\in \mathbb{R}^{q\times q}$ | Cholesky factor of $\mathbf{R}_k = \mathbf{S}_{\mathrm{R},k}\mathbf{S}_{\mathrm{R},k}^\mathrm{T}$ |
| $\mathbf{S}_{\mathrm{y},k}$ | $\in \mathbb{R}^{q\times q}$ | innovation error cov. matrix square-root |
| $\boldsymbol{\mathcal{X}}_{k-1}^+$ | $\in \mathbb{R}^{n\times 2n}$ | $\boldsymbol{\mathcal{S}}_{\boldsymbol{\mathcal{P}}}$ before passing through $\boldsymbol{f}_\mathrm{d}(\cdot)$ |
| $\boldsymbol{\mathcal{X}}_k^*$ | $\in \mathbb{R}^{n\times 2n}$ | $\boldsymbol{\mathcal{S}}_{\boldsymbol{\mathcal{P}}}$ after passing through $\boldsymbol{f}_\mathrm{d}(\cdot)$ |
| $\boldsymbol{\mathcal{X}}_k^-$ | $\in \mathbb{R}^{n\times 2n}$ | $\boldsymbol{\mathcal{S}}_{\boldsymbol{\mathcal{P}}}$ before passing through $\boldsymbol{h}_\mathrm{d}(\cdot)$ |
| $\boldsymbol{\mathcal{Y}}_k^*$ | $\in \mathbb{R}^{q\times 2n}$ | $\boldsymbol{\mathcal{S}}_{\boldsymbol{\mathcal{P}}}$ after passing through $\boldsymbol{h}_\mathrm{d}(\cdot)$ |
| $\mathbf{U}_k$ | $\in \mathbb{R}^{p\times 2n}$ | matrix with $2n$ column vectors of $\boldsymbol{u}_k$ |
| $\hat{\mathbf{X}}_{k-1}^+$ | $\in \mathbb{R}^{n\times 2n}$ | matrix with $2n$ column vectors of $\hat{\boldsymbol{x}}_{k-1}^+$ |
| $\hat{\mathbf{X}}_k^-$ | $\in \mathbb{R}^{n\times 2n}$ | matrix with $2n$ column vectors of $\hat{\boldsymbol{x}}_k^-$ |
| $\hat{\mathbf{Y}}_k$ | $\in \mathbb{R}^{q\times 2n}$ | matrix with $2n$ column vectors of $\hat{\boldsymbol{y}}_k$ |
| $\beta$ | $\in \mathbb{R}$ | collective blade pitch angle |
| $\dot{\varphi}_\mathrm{g}$ | $\in \mathbb{R}$ | generator angular speed |
| $\rho$ | $\in \mathbb{R}$ | air mass density |
| $M_\mathrm{g}$ | $\in \mathbb{R}$ | electrical generator torque |
| $v_\mathrm{w}$ | $\in \mathbb{R}$ | rotor effective wind speed |